

SIMULATION OF PERFLUOROMETHANE DECOMPOSITION IN AN ATMOSPHERIC-PRESSURE MICROWAVE DISCHARGE

A. P. Chernukho,^a A. N. Migun,^a
S. A. Zhdanok,^a J. C. Rostaing,^b
and J. Perrin^b

UDC 537.523.9, 539.1.04

The kinetic mechanism of transformation of perfluorohydrocarbons into the element system C–F–N–O has been investigated in detail. A two-dimensional stationary model of a reactor for decomposition of perfluoromethane under the conditions characteristic of a microwave discharge at atmospheric pressure is presented. Good agreement between the experimental and theoretical data has been obtained.

Introduction. In recent years, because of the introduction of stringent norms concerning the protection of the environment, problems on control and prevention of toxic effluents containing hotbed gases have become very pressing. It was established in the early 1990s that perfluorocompounds, such as CF₄, C₂F₆, SF₆, NF₃, are the most dangerous from the standpoint of the global rise in the temperature of the environment. Unlike the typical hotbed gases, such as CO₂ and CH₄, perfluorocompounds are more stable and have an average lifetime exceeding a thousand years (the lifetime of CF₄ is 50,000 years, and the lifetime of CO₂ is 120 years). Moreover, since perfluorocompounds have much larger absorption cross sections in the infrared region of the spectrum, as compared to the typical hotbed gases, their contribution to the global rise in the temperature of the environment can be 3–4 times larger than the contribution of, e.g., CO₂.

The semiconductor industry is one of the main sources of perfluorocompounds. The use of perfluorocompounds in this industry increases every year with increase in its power, which generates a need for the development of efficient methods of their reclamation. There are several methods of reclamation of perfluorocompounds with the use of an oxygen-containing plasma. Perfluorocompounds acted upon by this plasma are transformed into more light-weight oxygen-like compounds that are then caught in a gas cleaner. Problems on the use of different plasmas for reclamation of perfluorocompounds under various industrial conditions were described in detail in [1] with consideration for the specific energy expended for these purposes. It has been shown in this work that effluents containing no more than 0.1 volume percent of perfluorocompounds are most effectively purified with the use of a nonequilibrium plasma (plasma of corona or barrier discharges). The plasma of a microwave discharge is most appropriate for the case where the concentration of perfluorocompounds exceeds the above-indicated value (which is typical of the semiconductor industry) or a purification system of high capacity is required.

It is difficult to simulate a microwave discharge in detail, since, in this case, it is necessary to take into account a multitude of processes, such as propagation and absorption of electromagnetic waves in the gas, ionization of the gas, and formation and maintenance of the plasma. These problems are not an object of the present work because they were investigated in great depth in [2]. In the present work, most of our attention has been concentrated on the problem of simulation of the kinetics of transformation of perfluoromethane (CF₄) under the conditions of a microwave discharge [1].

Kinetic Model. The kinetic model developed includes 172 elementary chemical reactions and accounts for the formation and decomposition of 51 chemical elements: F, F₂, N, N₂, O, O₂, O₃, NO, NO₂, NO₃, N₂O, N₂O₃, N₂O₄, N₂O₅, NF, NF₂, NF₃, N₂F₂, N₂F₄, FO, FOO, F₂O, F₂O₂, NOF, NO₂F, C, C₂, C₃, CO, CO₂, C₂O, C₃O₂, CF, CF₂, CF₃, CF₄, C₂F₄, C₂F₅, C₂F₆, CN, CNN, CCN, C₂N₂, CNO, FCO, COF₂, CF₃O, CF₃OO, CF₃OF, CF₂CO, and FCCO.

^aA. V. Luikov Heat and Mass Transfer Institute, National Academy of Sciences of Belarus, 15 P. Brovka Str., Minsk, 220072, Belarus; email: chern@itmo.by; ^bAir Liquide Recherche et Development, France. Translated from *Inzhenerno-Fizicheskii Zhurnal*, Vol. 78, No. 2, pp. 178–188, March–April, 2005. Original article submitted September 30, 2004.

TABLE 1. General Data on the Mechanisms Considered

Mechanism	Number of components	Number of reactions	Number of problematic reactions	T_{\min} , K	T_{\max} , K
Konnov-05 [7]	127	1207	65	–	–
GRI-30 [8]	53	325	10	1000	3000
Miller–Bowman [9]	51	240	10	1500	6000
Frenklach [10]	99	533	51	2500	3500
Leeds [11]	37	175	12	2500	3000

Simulation of analogous systems (transformation of SF_6 in the plasma of a microwave discharge), carried out by us earlier [3], has shown that the influence of charged elements on the kinetics of the reaction is negligibly small and the decomposition process is thermal in character. Because of this, the kinetic model proposed in the present work contains only neutral chemical elements.

The temperature dependences of the thermodynamic properties of the elements considered were determined based mainly on the data of [4]. Some data were taken from [5] and [6]. To provide thermodynamic consistency of the system considered, data on the enthalpy of formation of elements under normal conditions were taken from one and the same source [6].

The kinetic mechanism was determined for the following conditions: (a) all the elementary reactions are reversible, (b) the exothermic direction of a reaction is its direct direction, (c) the rate constant of the direct reaction is defined by the modified Arrhenius relation and the rate constant of the inverse reaction is determined in accordance with the principle of detailed balancing, and (d) the reactions in which a third body (particle M) participate can occur at limiting low and high pressures matched by the Lindemann method.

The rate constants of certain reactions in a number of temperature ranges, calculated in accordance with the principle of detailed balancing in the process of investigation of the kinetic mechanism, turned out to be overestimated and contradictory to the kinetic theory of collisions (it is known from the kinetic theory that the rate constant of an elementary bimolecular reaction between neutral elements cannot exceed $\approx 10^{-9} \text{ cm}^3/\text{sec}$ and the rate constant of an analogous trimolecular reaction is $\approx 10^{-26} \text{ cm}^6/\text{sec}$). The above-indicated excess is characteristic of reactions with a high activation barrier and is explained by the fact that, in experiments, the rate constant of a reaction is measured in a limiting temperature range. For example, the rate constants of dissociation reactions are usually measured at fairly high temperatures. In this case, even a small error in determining the activation energy can result in the dissociation rate constant being overestimated or underestimated by many orders of magnitude. The recombination rate constant calculated in this temperature range in accordance with the principle of detailed balancing will be overestimated or underestimated by the same value. In the case of overestimating, it can exceed the value corresponding to the gas-kinetic frequency of collisions and will lose any physical meaning. This does not influence the calculation of the dissociation rate since the thermal-dissociation rate is practically equal to zero at low temperatures, but it can lead to a very large error in calculating the recombination rate under certain conditions.

Because of this, we verified the rate constants of widely used kinetic mechanisms of oxidation of hydrocarbons. It has been established that practically all of the mechanisms considered have incorrectly determined rate constants contradictory to the kinetic theory of collisions. The results of verification are presented in Table 1. The last two columns present the temperatures at which all the rate constants used in the kinetic scheme are not contradictory to the kinetic theory. It is seen that almost all tested mechanisms have a fairly narrow temperature interval in which all the reaction-rate constants are determined correctly, and this range is absent in the mechanism of A. Konnov.

It should be noted that this fact is not evidence of the incorrectness of the mechanisms on the whole, since they are used to advantage for simulation of various physicochemical systems. The indicated incorrectness in determining the rate constants can lead to significant errors in calculating the kinetics only under certain conditions where the products of an incorrectly determined reaction can get to the region with the temperature at which the above-indicated effect appears. Such conditions can arise when a hot gas mixture is rapidly cooled, in the case of existence of large temperature inhomogeneities where there can arise a diffusion transfer of components from the hot zone to the cold zone, in the case of expansion of the gas in supersonic nozzles, and in other cases.

To avoid the above-described incorrectnesses in determining the kinetic mechanism of the reaction studied we used the exothermic channel as the direct reaction channel. Moreover, the Arrhenius expression for the rate constant was obtained in a number of cases with the use of the data for both the direct and inverse channels. Thus, the kinetic mechanism constructed in the present work is free of the above-described incorrectnesses in determining the rate constants.

Table 2 presents a complete list of reactions involved in the kinetic mechanism considered as well as the corresponding rate constants, literature sources, and commentaries. The rate constants were calculated by the modified Arrhenius expression.

$$k = AT^\beta \exp\left(-\frac{E_a}{T}\right).$$

Mathematical Model. The design of the reactor used in the present work was described in detail in [1]. It consists of a cooled discharge tube in which a treated gas flows. A waveguide crosses the tube at its center. At the intersection a high-temperature plasma is formed. The gas passed through the reactor enters a heat exchanger, where it is cooled completely.

The initial conditions and reactor parameters used for simulation of the reaction studied were as follows: discharge-tube length, 300 mm; discharge-tube diameter, 8 mm; afterdischarge-tube diameter, 12 mm; gas flow rate, 20–60 liters/min; discharge power, 3–5.1 kW; initial mixture composition, $N_2:O_2:CF_4 = 100-2.5\gamma:1.5\gamma:\gamma$, $\gamma = 0.1-1.0$.

The mathematical model was developed for the case where (1) the system has a cylindrical geometry, (2) the entire energy of the microwave discharge is expended in heating the gas flow, and (3) the length of the discharge region and the radial energy distribution (taken from [2]) are the input parameters.

Assumption (2) is correct since a microwave discharge is characterized by a low reduced electric field strength and a low characteristic electron temperature. Under these conditions, practically all of the energy transferred from the field to the electrons is expended in excitation of the rotational and translational degrees of freedom of molecules.

The problem was mathematically formulated in the form of a system of differential equations:

$$c_p \rho u \frac{\partial T}{\partial x} + \frac{1}{r} \frac{\partial}{\partial r} \left(r \rho \sum_i Y_i V_i h_i \right) - \frac{1}{r} \frac{\partial}{\partial r} \left(r \lambda \frac{\partial T}{\partial r} \right) + \sum_i \dot{\omega}_i h_i - W = 0, \quad (1)$$

$$\rho u \frac{\partial Y_i}{\partial x} + \frac{1}{r} \frac{\partial}{\partial r} (r \rho Y_i V_i) = \dot{\omega}_i \mu_i, \quad i = 1, \dots, N, \quad (2)$$

$$\rho u = \text{const}, \quad (3)$$

$$p(x, r) = p_0 = \text{const}, \quad (4)$$

$$\rho = p \frac{\mu}{RT}. \quad (5)$$

Here (1) is the energy-conservation equation, (2) and (3) represent the mass-conservation and mass-continuity laws, Eq. (4) defines the isobaric properties of the system, and (5) represents the equation of an ideal-gas state.

As is seen from system (1)–(5), the model does not take into account the gas diffusion and heat transfer in the longitudinal direction, since, because of the high velocity of the gas flow, convection significantly dominates the other processes of transfer in the axial direction.

Estimation of the typical operating conditions of the reactor has shown that the Reynolds number Re of a cold gas can be as high as 10,000, which corresponds to the purely turbulent flow conditions. At the same time, Re

TABLE 2. Kinetic Mechanism

No. in order	Reaction [efficiency of the third particle]	Limit	M	A (m)	β	E_a	Lit. source	Commentary
1	2	3	4	5	6	7	8	9
1	$\text{CF}_3 + \text{F}(\text{+M}) \rightleftharpoons \text{CF}_4(\text{+M})$	HP LP	Ar	2.7 (-14) 3.0 (-22)	-7.9 -3.04	4504 -1545	[12] [6]	b
2	$\text{CF}_2 + \text{F}(\text{+M}) \rightleftharpoons \text{CF}_3(\text{+M})$	HP LP	Ar	2.0 (-11) 4.0 (-33)	0 0	0 -2465	[6] [6]	b
3	$\text{CF}_3 + \text{O} \rightleftharpoons \text{COF}_2 + \text{F}$			3.3 (-11)	0	0	[6, 12]	
4	$\text{COF}_2 + \text{F}(\text{+M}) \rightleftharpoons \text{CF}_3\text{O}(\text{+M})$ [CO/1.5/CO ₂ /2/Ar/0.7/]	HP		4.2 (-12)	0	4076	[6]	
5	$\text{CF}_3\text{O} + \text{F} \rightleftharpoons \text{COF}_2 + \text{F}_2$			1.0 (-10)	0	0	[13]	
6	$\text{CF}_3 + \text{O}_2(\text{+M}) \rightleftharpoons \text{CF}_3\text{OO}(\text{+M})$	HP LP		1.0 (-11) 1.2 (-31)	0 0	0 -1499	[6] [6]	b
7	$\text{CF}_3 + \text{O}_2 \rightleftharpoons \text{CF}_3\text{O} + \text{O}$			8.8 (-12)	0	8852	[6]	b
8	$\text{CF}_3 + \text{NO}_2 \rightleftharpoons \text{CF}_3\text{O} + \text{NO}$			5.0 (-12)	0	0	[6]	
9	$\text{CF}_3 + \text{NO}_2 \rightleftharpoons \text{COF}_2 + \text{NOF}$			1.1 (-11)	0	0	[6]	
10	$\text{CF}_3 + \text{N}_2\text{O} \rightleftharpoons \text{CF}_3\text{O} + \text{N}_2$			2.3 (-11)	0	12,077	[6]	
11	$\text{CF}_3 + \text{O}_3 \rightleftharpoons \text{CF}_3\text{O} + \text{O}_2$			1.0 (-12)	0	0	[6]	
12	$\text{CF}_3 + \text{F}_2 \rightleftharpoons \text{CF}_4 + \text{F}$			4.4 (-12)	0	1263	[6]	
13	$\text{CF}_3 + \text{CF}_2(\text{+M}) \rightleftharpoons \text{C}_2\text{F}_5(\text{+M})$	HP LP		1.6 (-11) 2.3 (-26)	0 0	808 0	[6] [6]	
14	$2\text{CF}_3(\text{+M}) \rightleftharpoons \text{C}_2\text{F}_6(\text{+M})$	HP LP		2.7 (-12) 1.6 (-28)	-7.26 0	3548 1124	[12] [6]	b
15	$\text{CF}_3 + \text{CF}_3\text{OF} \rightleftharpoons \text{CF}_4 + \text{CF}_3\text{O}$			3.3 (-16)	0	0	[6]	
16	$\text{CF} + \text{F}(\text{+M}) \rightleftharpoons \text{CF}_2(\text{+M})$	HP LP		1.0 (-11) 3.0 (-31)	0 0	0 0	[6] [6]	
17	$\text{CF}_2 + \text{O} \rightleftharpoons \text{FCO} + \text{F}$			1.2 (-10)	0	503	[12]	
18	$\text{CF}_2 + \text{O}_2 \rightleftharpoons \text{COF}_2 + \text{O}$			2.2 (-11)	0	13,192	[6]	
19	$\text{CF}_2 + \text{NO}_2 \rightleftharpoons \text{COF}_2 + \text{NO}$			7.5 (-15)	0	0	[6]	
20	$\text{CF}_2 + \text{F}_2 \rightleftharpoons \text{CF}_3 + \text{F}$			1.0 (-15)	0	0	[6]	
21	$2\text{CF}_2(\text{+M}) \rightleftharpoons \text{C}_2\text{F}_4(\text{+M})$ [CO/1.5/CO ₂ /2/Ar/0.7/]	HP		1.1 (-10)	0	2547	[6]	
22	$\text{CF} + \text{O} \rightleftharpoons \text{CO} + \text{F}$			6.6 (-11)	0	503	[12]	
23	$\text{CF} + \text{O}_2 \rightleftharpoons \text{FCO} + \text{O}$			3.3 (-11)	0	906	[12]	
24	$\text{CF} + \text{N} \rightleftharpoons \text{CN} + \text{F}$			3.4 (-12)	0	0	[6]	
25	$\text{CF}_3\text{O} + \text{O}_2 \rightleftharpoons \text{COF}_2 + \text{FOO}$			1.0 (-10)	0	5600	[6]	
26	$\text{CF}_3\text{O} + \text{CO} \rightleftharpoons \text{CF}_3 + \text{CO}_2$			4.0 (-16)	0	0	[6]	
27	$\text{CF}_3\text{O} + \text{CO} \rightleftharpoons \text{COF}_2 + \text{FCO}$			2.0 (-15)	0	0	[6]	
28	$\text{CF}_3\text{O} + \text{NO} \rightleftharpoons \text{COF}_2 + \text{NOF}$			3.7 (-11)	0	-110	[6]	
29	$\text{CF}_3\text{O} + \text{NO}_2 \rightleftharpoons \text{COF}_2 + \text{NO}_2\text{F}$			3.2 (-12)	0	0	[6]	
30	$\text{CF}_3\text{O} + \text{F} \rightleftharpoons \text{CF}_3\text{OF}$			5.8 (-11)	0	0	[6]	
31	$\text{CF}_3\text{O} + \text{O}_3 \rightleftharpoons \text{CF}_3\text{OO} + \text{O}_2$			2.0 (-12)	0	1300	[6]	
32	$\text{C} + \text{O} + \text{M} \rightleftharpoons \text{CO} + \text{M}$			2.0 (-34)	0	0	[6]	
33	$\text{C} + \text{O}_2 \rightleftharpoons \text{O} + \text{CO}$			9.6 (-11)	0	290	[12]	
34	$\text{C} + \text{C}_2\text{N}_2 \rightleftharpoons \text{CN} + \text{CCN}$			3.0 (-11)	0	0	[6]	
35	$\text{C}_2 + \text{N} \rightleftharpoons \text{C} + \text{CN}$			5.0 (-10)	0	0	[6]	i
36	$\text{C} + \text{CO} + \text{M} \rightleftharpoons \text{C}_2\text{O} + \text{M}$			6.3 (-32)	0	0	[6]	
37	$\text{C} + \text{CO}_2 \rightleftharpoons 2\text{CO}$			1.0 (-16)	0	0	[6]	
38	$\text{C} + \text{N} + \text{M} \rightleftharpoons \text{CN} + \text{M}$			9.4 (-33)	0	0	[6]	
39	$\text{C} + \text{NO} \rightleftharpoons \text{CN} + \text{O}$			3.3 (-11)	0	0	[6]	
40	$\text{C} + \text{NO} \rightleftharpoons \text{CO} + \text{N}$			4.7 (-11)	0	0	[6, 7]	
41	$\text{C} + \text{N}_2 + \text{M} \rightleftharpoons \text{CNN} + \text{M}$			3.1 (-33)	0	0	[6, 7]	
42	$\text{C} + \text{N}_2\text{O} \rightleftharpoons \text{CN} + \text{NO}$			8.0 (-12)	0	0	[6, 7]	
43	$\text{C} + \text{F}_2 \rightleftharpoons \text{CF} + \text{F}$			2.8 (-12)	0	754	[6]	
44	$2\text{C}(\text{+M}) \rightleftharpoons \text{C}_2(\text{+M})$	HP LP		2.2 (-11) 2.2 (-33)	0 0	0 -2000	[6] [6]	d

TABLE 2

Continued

1	2	3	4	5	6	7	8	9
45	$C_2 + O \rightleftharpoons CO + C$			6.0 (-10)	0	0	[6, 7]	
46	$C_2 + O_2 \rightleftharpoons 2CO$			1.5 (-11)	0	493	[7]	
47	$2C_2 \rightleftharpoons C_3 + C$			5.3 (-10)	0	0	[6]	
48	$C_2 + N_2 \rightleftharpoons 2CN$			2.5 (-11)	0	21,000	[7]	
49	$CN + O \rightleftharpoons CO + N$			3.2 (-12)	0.46	364	[6, 7]	
50	$CN + O_2 \rightleftharpoons NCO + O$			1.2 (-11)	0	-201	[7]	
51	$2CN(+M) \rightleftharpoons C_2N_2(+M)$	HP LP		9.4 (-12)	0	0	[6]	
			N ₂	9.4 (-23)	-2.61	0	[6]	
52	$CN + NCO \rightleftharpoons CNN + CO$			3.0 (-11)	0	0	[6, 7]	
53	$CN + CO_2 \rightleftharpoons NCO + CO$			1.6 (-11)	0	1956	[6]	g
54	$CN + N \rightleftharpoons N_2 + C$			1.0 (-10)	0	0	[6]	
55	$CN + N + M \rightleftharpoons CNN + M$		N ₂	2.8 (-32)	0	0	[6]	
56	$NCO + N \rightleftharpoons CN + NO$			4.5 (-6)	-0.99	8655	[7]	
57	$CN + NO \rightleftharpoons N_2 + CO$			1.4 (-11)	0	1496	[6]	
58	$CN + NO_2 \rightleftharpoons NCO + NO$			8.8 (-9)	-0.75	173	[7]	
59	$CN + NO_2 \rightleftharpoons CO_2 + N_2$			6.1 (-10)	-0.75	173	[7]	
60	$CN + NO_2 \rightleftharpoons CO + N_2O$			8.2 (-10)	-0.75	173	[7]	
61	$CN + N_2O \rightleftharpoons NCO + N_2$			1.0 (-11)	0	7730	[7]	
62	$CN + N_2O \rightleftharpoons CNN + NO$			6.4 (-21)	2.6	1860	[6]	
63	$CNN + O \rightleftharpoons CO + N_2$			1.7 (-11)	0	0	[7]	
64	$CNN + O \rightleftharpoons CN + NO$			1.7 (-10)	0	10,064	[7]	
65	$CNN + O_2 \rightleftharpoons NO + NCO$			1.7 (-11)	0	2516	[7]	
66	$CCN + O \rightleftharpoons CO + CN$			6.00 (-12)	0	0	[6]	
67	$CCN + N \rightleftharpoons 2CN$			1.0 (-10)	0	0	[6]	
68	$C_2N_2 + O \rightleftharpoons CN + NCO$			7.6 (-12)	0	4470	[7]	
69	$NCO + M \rightleftharpoons N + CO + M$			3.7 (-10)	0	27,200	[7]	
70	$NCO + O \rightleftharpoons CO + NO$			7.5 (-11)	0	0	[7]	
71	$NCO + O \rightleftharpoons N + CO_2$			1.3 (-11)	0	1258	[7]	
72	$NCO + O_2 \rightleftharpoons NO + CO_2$			2.3 (-12)	0	10,064	[7]	
73	$2NCO \rightleftharpoons 2CO + N_2$			4.3 (-11)	0	549	[6]	b
74	$NCO + N \rightleftharpoons N_2 + CO$			3.3 (-11)	0	0	[6, 7]	
75	$NCO + NO \rightleftharpoons CO + N_2 + O$			7.6 (-12)	0	0	[6]	
76	$NCO + NO \rightleftharpoons CO + N_2O$			7.6 (-6)	-2.0	470	[7]	
77	$NCO + NO \rightleftharpoons N_2 + CO_2$			9.6 (-6)	-2.0	470	[7]	
78	$NCO + NO_2 \rightleftharpoons 2NO + CO$			4.7 (-11)	-0.65	-164	[7]	
79	$NCO + NO_2 \rightleftharpoons N_2O + CO_2$			5.9 (-10)	-0.65	-164	[7]	
80	$NCO + N_2O \rightleftharpoons N_2 + NO + CO$			5.0 (-12)	0	0	[7]	
81	$NCO + F \rightleftharpoons NF + CO$			9.2 (-12)	0	0	[6]	
82	$FCO + O \rightleftharpoons CO_2 + F$			5.0 (-11)	0	0	[12]	
83	$FCO + F(+M) \rightleftharpoons COF_2(+M)$	HP LP		1.7 (-12)	0	0	[12]	
				2.7 (-22)	-3.0	0	[6]	d
84	$FCO + F_2 \rightleftharpoons COF_2 + F$			1.1 (-11)	0	1630	[6]	b
85	$2FCO \rightleftharpoons COF_2 + CO$			3.7 (-11)	0	160	[6, 12]	
86	$FCO + O_2 \rightleftharpoons CO_2 + F + O$			3.3 (-11)	0	12,077	[12]	
87	$C_2O + CO + M \rightleftharpoons C_3O_2 + M$		Ar	2.0 (-23)	-3.5	0	[6]	i
88	$C_3O_2 + O \rightleftharpoons C_2O + CO_2$			4.1 (-14)	0	0	[6]	
89	$CO + O(+M) \rightleftharpoons CO_2(+M)$ [CO/1.9/CO ₂ /3.8/Ar/0.9/]	HP		2.7 (-14)	0	1459	[6]	
90	$CO + F(+M) \rightleftharpoons FCO(+M)$ [CO/1.5/CO ₂ /2/Ar/0.7/]	LP		5.5 (-13)	0	0	[6]	
91	$CO + O_2 \rightleftharpoons CO_2 + O$			4.2 (-12)	0	24,054	[7, 12]	
92	$CO + N_2O \rightleftharpoons CO_2 + N_2$			4.2 (-10)	0	23,148	[7]	
93	$CO + NO_2 \rightleftharpoons CO_2 + NO$			1.5 (-10)	0	17,009	[7]	

TABLE 2

Continued

1	2	3	4	5	6	7	8	9
94	CO + FO \rightleftharpoons CO ₂ + F			1.3 (-13)	0	0	[6]	
95	CO + F ₂ \rightleftharpoons FCO + F			4.0 (-10)	0	9500	[6]	d
96	CO + F ₂ O \rightleftharpoons FCO + FO			4.6 (-11)	0	12,530	[6]	
97	CO ₂ + N \rightleftharpoons CO + NO			3.2 (-13)	0	1710	[6, 7]	
98	C ₂ O + O \rightleftharpoons 2CO			8.6 (-11)	0	0	[6, 7]	
99	C ₂ O + O ₂ \rightleftharpoons 2CO + O			3.3 (-11)	0	0	[7]	
100	C ₂ O + O ₂ \rightleftharpoons CO + CO ₂			3.3 (-11)	0	0	[7]	
101	CF ₃ OO + CO \rightleftharpoons CF ₃ O + CO ₂			5.0 (-16)	0	0	[6]	
102	C ₂ F ₄ + O \rightleftharpoons CF ₂ + COF ₂			3.2 (-15)		0	[12]	
103	CF ₂ CO + O \rightleftharpoons COF ₂ + CO			1.7 (-11)	0	4026	[12]	
104	FCCO + F \rightleftharpoons CF ₂ + CO			5.0 (-11)	0	0	[12]	
105	FCCO + O \rightleftharpoons FCO + CO			1.7 (-10)	0	0	[12]	
106	C ₂ F ₄ + F \rightleftharpoons CF ₃ + CF ₂			5.0 (-11)	0	0	[12]	
107	F + O ₂ (+M) \rightleftharpoons FOO(+M)	HP LP	N ₂	2.4 (-13) 1.1 (-30)	0 -1.0	0 0	[6] [6]	
108	F + F ₂ O ₂ \rightleftharpoons FOO + F ₂			3.6 (-14)	0	0	[6]	
109	F + NO(+M) \rightleftharpoons NOF(+M)	HP LP		1.0 (-11) 8.3 (-32)	0 0	0 0	[6] [6]	
110	F + FOO(+M) \rightleftharpoons F ₂ O ₂ (+M)	HP LP		8.8 (-13) 3.0 (-32)	0 0	0 0	[6] [6]	
111	F + NF ₂ (+M) \rightleftharpoons NF ₃ (+M)	HP LP	N ₂	4.7 (-17) 1.6 (-33)	0 0	-3722 -2298	[6] [6]	b b
112	F + F ₂ O \rightleftharpoons FO + F ₂			8.5 (-14)	0	6894	[6]	
113	F + NO ₃ \rightleftharpoons FO + NO ₂			3.0 (-11)	0	0	[6]	
114	F ₂ + O \rightleftharpoons FO + F			4.3 (-15)	0	1154	[6]	b
115	F ₂ + NO \rightleftharpoons NOF + F			6.9 (-13)	0	1150	[6]	
116	F ₂ + NO ₂ \rightleftharpoons NO ₂ F + F			2.6 (-12)	0	5268	[6]	
117	F ₂ + NF ₂ \rightleftharpoons NF ₃ + F			4.3 (-12)	0	6493	[6]	b
118	FO + O \rightleftharpoons F + O ₂			2.7 (-11)	0	0	[6]	
119	FO + N \rightleftharpoons F + NO			2.0 (-11)	0	0	[6]	a
120	FO + N \rightleftharpoons O + NF			6.0 (-12)	0	0	[6]	a
121	FO + NO \rightleftharpoons NO ₂ + F			8.2 (-12)	0	-300	[6]	
122	2FO \rightleftharpoons 2F + O ₂			1.0 (-11)	0	0	[6]	
123	2FO \rightleftharpoons F + FOO			5.0 (-13)	0	0	[6]	
124	FO + NF ₂ \rightleftharpoons 2F + NOF			3.8 (-12)	0	0	[6]	
125	FO + NO ₃ \rightleftharpoons FOO + NO ₂			1.0 (-12)	0	0	[6]	
126	FOO + O \rightleftharpoons FO + O ₂			5.0 (-11)	0	0	[6]	
127	F ₂ + O + M \rightleftharpoons F ₂ O + M			1.1 (-18)	-4.03	0	[6]	c
128	F ₂ O + NF ₂ \rightleftharpoons NF ₃ + FO			5.1 (-12)	0.5	11,121	[6]	
129	2NF \rightleftharpoons 2F + N ₂			3.5 (-12)	0	0	[6]	
130	F + NF + M \rightleftharpoons NF ₂ + M		Ar	3.4 (-21)	-3.62	0	[6]	c
131	NF ₂ + O \rightleftharpoons F + NOF			1.3 (-11)	0	0	[6]	
132	NF + FO \rightleftharpoons NF ₂ + O			1.0 (-11)	0	0	[6]	h
133	NF ₂ + N \rightleftharpoons 2NF			3.0 (-12)	0	0	[6]	
134	NF ₂ + NO ₂ \rightleftharpoons 2NOF			8.6 (-14)	0	2450	[6]	
135	2NF ₂ \rightleftharpoons NF ₃ + NF			1.7 (-12)	0	18,594	[6]	
136	2O + M \rightleftharpoons O ₂ + M		Ar	2.8 (-31)	-1.0	0	[6, 7]	
	[O/71/O ₂ /20/NO/5/N ₂ /5/N/5/]							
137	N ₂ + O \rightleftharpoons NO + N			3.0 (-10)	0	38,300	[6, 7]	
138	N + O ₂ \rightleftharpoons NO + O			1.5 (-14)	1.0	3270	[6, 7]	
139	N + O + M \rightleftharpoons NO + M		N ₂	1.1 (-33)	0	0	[6]	i
140	2NO \rightleftharpoons N ₂ + O ₂			2.5 (-11)	0	30,653	[6]	b
141	N ₂ O(+M) \rightleftharpoons N ₂ + O(+M)	HP		1.3 (12)	0	31,511	[7]	

TABLE 2

Continued

1	2	3	4	5	6	7	8	9
	[O ₂ /1.4/N ₂ /1.7/NO/3/N ₂ O/3.5/]							
142	N ₂ O + O ⇌ N ₂ + O ₂			1.7 (-10)	0	14,191	[6, 7]	b
143	N ₂ O + O ⇌ 2NO			1.2 (-10)	0	13,401	[6, 7]	b
144	N ₂ O + N ⇌ N ₂ + NO			1.7 (-11)	0	10,064	[7]	
145	N ₂ O + NO ⇌ N ₂ + NO ₂			4.6 (-10)	0	25,161	[6, 7]	
146	NO + O(+M) ⇌ NO ₂ (+M)	HP		2.2 (-9)	-0.75	0	[7]	
	[NO ₂ /6/NO/1.8/O ₂ /0.8/ N ₂ O/4.4/CO ₂ /1.25/Ar/0.6/]							
147	NO ₂ + O ⇌ NO + O ₂			6.5 (-12)	0	-120	[6, 7]	
148	NO ₂ + N ⇌ N ₂ O + O			1.4 (-12)	0	0	[7]	
149	NO ₂ + N ⇌ 2NO			1.7 (-12)	0	0	[7]	
150	NO ₂ + NO ⇌ N ₂ O + O ₂			1.7 (-12)	0	30,193	[7]	
151	2NO ₂ ⇌ 2NO + O ₂			6.6 (-12)	0	13,884	[6]	b
152	NO ₃ + NO ⇌ 2NO ₂			1.8 (-11)	0	-110	[6]	
153	NO ₂ + O(+M) ⇌ NO ₃ (+M)	HP		2.2 (-11)	0	0	[6, 7]	
	[O ₂ /0.8/CO ₂ /2.6/]	LP	N ₂	4.1 (-20)	-4.08	1242	[6, 7]	
154	NO ₃ (+M) ⇌ NO + O ₂ (+M)	HP		2.5 (6)	0	6099	[6, 7]	
		LP		4.5 (-13)	0	2113	[6]	b
155	NO ₃ + NO ₂ ⇌ NO + NO ₂ + O ₂			2.0 (-13)	0	1610	[6, 7]	b
156	NO ₃ + O ⇌ NO ₂ + O ₂			1.7 (-11)	0	0	[6, 7]	
157	2NO ₃ ⇌ 2NO ₂ + O ₂			8.5 (-13)	0	2451	[6, 7]	b
158	N ₂ O ₄ (+M) ⇌ 2NO ₂ (+M)	HP		4.1 (18)	-1.1	6461	[7]	
		LP	N ₂	3.3 (4)	-3.8	6461	[7]	
159	N ₂ O ₄ + O ⇌ N ₂ O ₃ + O ₂			2.0 (-12)	0	0	[7]	
160	NO ₂ + NO(+M) ⇌ N ₂ O ₃ (+M)	HP		2.7 (-15)	1.4	0	[7]	
		LP	N ₂	3.8 (-15)	-7.7	0	[7]	
161	N ₂ O ₃ + O ⇌ 2NO ₂			4.5 (-13)	0	0	[7]	
162	2N + M ⇌ N ₂ + M		N ₂	1.4 (-33)	0	-503	[6]	
	[N/5/O/2.2/]							
163	2F + M ⇌ F ₂ + M		Ar	3.8 (-29)	-2.0	515	[6]	
164	NF + N ₂ F ₂ ⇌ NF ₂ + N ₂ + F							
165	NF ₂ + NF ⇌ N ₂ F ₂ + F			2.4 (-12)	0	0	[6]	
166	NF ₂ + NF ₂ (+M) ⇌ N ₂ F ₄ (+M)	HP		3.0 (-13)	0	0	[6]	i
		LP		1.0 (-32)	0	0	[6]	
167	NO ₂ + NO ₃ (+M) ⇌ N ₂ O ₅ (+M)	HP		2.0 (-12)	0	0	[6]	
		LP		1.3 (-21)	-3.5	0	[6]	
168	CF ₂ + N ⇌ FCN + F			7.2 (-12)	0	0	[6]	a
169	CF ₃ + CF ₂ ⇌ CF ₄ + CF			1.0 (-14)	0	0	[6]	a, i
170	C ₂ N ₂ + N ⇌ CCN + N ₂			1.0 (-11)	0	0	[6]	a
171	FCO + NO ⇌ NOF + CO			5.7 (-14)	0	0	[6]	a
172	C ₃ O ₂ + F ⇌ FCCO + CO			9.3 (-11)	0	440	[6]	a

Notes. M, third particle; LP, low pressure; HP, high pressure; $A \cdot 10^m$; a, reaction products are absent in the literature source; b, best approximation of the data of [6]; c, approximation of the data calculated by the inverse constants; d, combined approximation of the data by the direct and inverse constants; e, best approximation of the recent data of [6]; f, efficiency of the third particles in various components taken from [12]; g, best approximation of all the experimental data from [6]; h, constant obtained from the inverse constant calculated at 2000 K; i, direct constant calculated by the inverse constant.

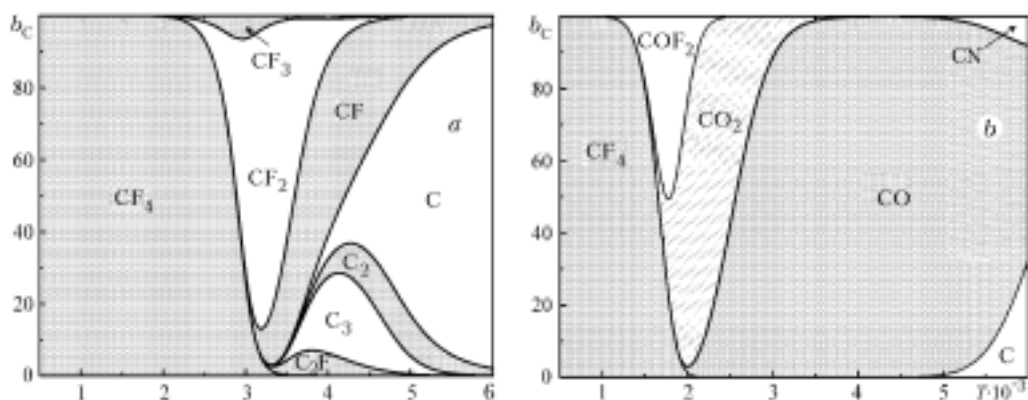


Fig. 1. Balance of carbon atoms in pure perfluoromethane (a) and the mixture $N_2:O_2:CF_4 = 97.5:1.5:1.0$ (b) under equilibrium conditions at normal pressure. b_C , %; T , K.

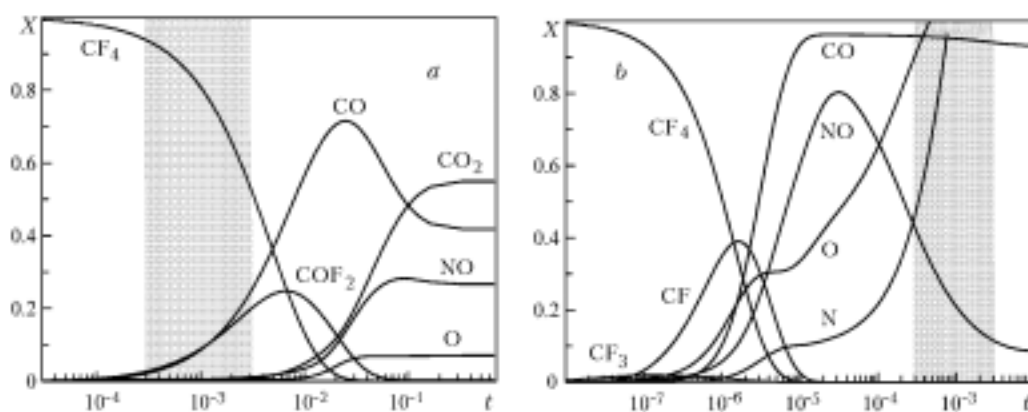


Fig. 2. Change in the concentration of the main components in the process of isothermal decomposition of perfluoromethane: $T = 2500$ K (a) and 5000 (b). The initial mixture is $N_2:O_2:CF_4 = 97.5:1.5:1.0$. The shaded regions correspond to the characteristic times of residence of gas in the discharge zone of the reactor. X , %; t , sec.

of the gas in the high-temperature discharge region can be as low as 1000–2000, which corresponds to the transient regime of flow. Such behavior of the Reynolds number is explained by the fact that the viscosity of nitrogen, which is the largest constituent of the mixture, anomalously increases with increase in the temperature. As is known, simulation of transient regimes of flow represents a very complex problem even for nonreacting systems. Because of this, for the purpose of simplification of the model, we did not consider the equation of motion in this formulation, just as in [2]; instead, different radial gas-velocity distributions were determined. These distributions were assumed to be steady-state (turbulent or laminar) and were normalized to the total mass flow rate of the mixture.

Results of Simulation. Analysis of the thermodynamic properties of perfluoromethane has shown that it is a very stable compound resistant to high temperatures. Pure perfluoromethane, on being heated, remains stable (see Fig. 1a) up to temperatures of 2000–2500 K (hereinafter we present results obtained at atmospheric pressure). It is completely decomposed at a temperature higher than 3400 K. However, even a temperature of 6000 K is insufficient to completely decompose all the CF_n compounds. On addition of oxygen, the thermal stability threshold of CF_4 decreases to ~ 1200 K (see Fig. 1b). In this case, it can be completely decomposed even at $T > 2000$ K. In this case, the main potential products of the CF_4 transformation are oxygen-containing molecules: COF_2 , CO_2 , and CO . It is in this orderly sequence in which they appear in an equilibrium mixture when the temperature increases. At temperatures higher than 5000 K, large amounts of CN and C appear among the decomposition products. However, the main carbon-containing substance in an equilibrium plasma at temperatures ranging from 3000 to 6000 K is CO .

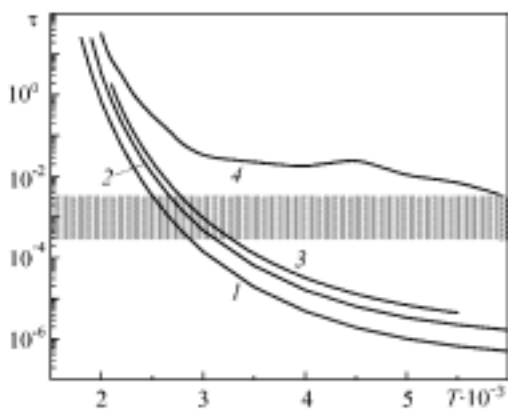


Fig. 3. Dependence of the characteristic time of isothermal decomposition of perfluoromethane on the temperature: 50 (1), 10 (2), and 1% of the initial concentration (3); 4) characteristic time of establishment of the equilibrium. The initial mixture is $N_2:O_2:CF_4 = 97.5:1.5:1.0$. The shaded region corresponds to the characteristic time of residence of gas in the discharge region of the reactor. τ , sec; T , K.

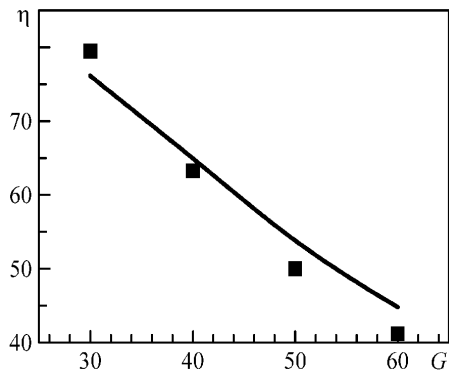


Fig. 4. Experimental (points) and calculation (curve) dependences of the efficiency of purification of the gas mixture on its flow rate at a discharge power of 4 kW. The initial mixture is $N_2:O_2:CF_4 = 99.75:0.15:0.1$. η , %; G , liters/min.

In actual practice, the mixture of decomposition products is not in equilibrium. This is mainly explained by the limited time of residence of the gas mixture in the hot zone of the reactor. Figure 2 shows the results of simulation of the kinetics of isothermal decomposition of perfluoromethane at 2500 and 5000 K. The calculations were carried out for a typical mixture used in apparatus for reclamation of perfluoromethane: $N_2:O_2:CF_4 = 97.5:1.5:1.0$. The characteristic time of residence of gas in the discharge region of such an apparatus operating under typical conditions is $3 \cdot 10^{-4}$ – $3 \cdot 10^{-3}$ sec. It is seen that at a temperature of 2500 K the residence time is insufficient even for a half decomposition of perfluoromethane, while at a temperature of 5000 K the residence time exceeds the time necessary for the complete decomposition of perfluoromethane by an order of magnitude.

Figure 3 shows the dependence of the characteristic time of decomposition of CF_4 on the temperature. It is seen that this compound is effectively decomposed at temperatures exceeding 3000 K. Note that the time required for obtaining an equilibrium composition of products is several orders of magnitude larger than the time required for the decomposition of CF_4 (curve 4 in Fig. 2). This is mainly explained by the chemical transformations of the perfluoromethane decomposition products. At high temperatures ($T > 5000$ K), the attainment of an equilibrium state is limited by the dissociation of nitrogen, which constitutes the main part of the mixture.

In actual practice, the gas flow in the discharge region is very inhomogeneous in the radial direction due to the specific heating of the gas flow by the microwave discharge and simultaneous cooling of the discharge tube for the purpose of preventing its damage. Along with the central high-temperature region of the flow (in which the temperature can reach 5000–6000 K), where the decomposition process proceeds very rapidly [14], there exist cold near-wall regions where chemical reactions are practically absent. This spatial inhomogeneity mainly prevents the complete decomposition of perfluoromethane even at high specific energies supplied to the discharge. The indicated effect is partially compensated by the radial diffusion that transports reagents from the cold near-wall regions to the hot regions of the flow. However, the total positive effect of this process does not exceed 10–15%.

The data of our numerical calculations are in good agreement with the corresponding experimental data [1], which is evidence of the adequacy of the kinetic model developed. By way of example, Fig. 4 shows experimental and calculated dependences of the efficiency of perfluoromethane decomposition on the gas-mixture flow rate at a constant discharge power (4000 W).

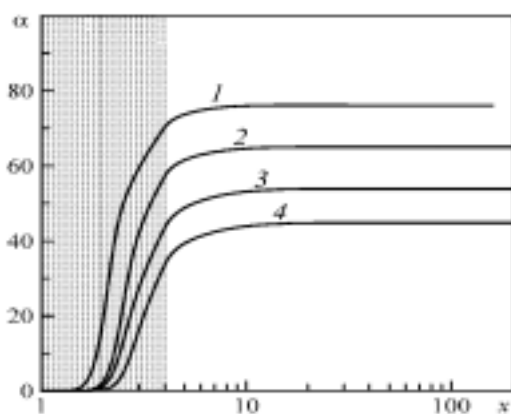


Fig. 5. Dynamics of decomposition of perfluoromethane in the initial mixture $N_2:O_2:CF_4 = 99.75:0.15:0.1$ at a discharge power of 4 kW and a gas-flow rate $G = 30$ (1), 40 (2), 50 (3), and 60 liters/min (4). The shaded region corresponds to the discharge zone of the reactor. α , %; x , cm.

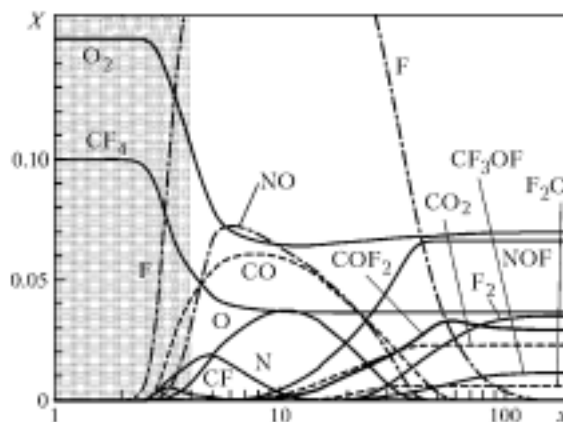


Fig. 6. Dynamics of change in the concentration of the main components of the initial mixture $N_2:O_2:CF_4 = 99.75:0.15:0.1$ in the discharge and afterdischarge zones of the reactor at a discharge power of 4 kW and a gas-flow rate of 40 liters/min. The shaded region corresponds to the discharge zone of the reactor. X , %; x , cm.

Figure 5 presents the calculated dynamics of the CF_4 decomposition along the axis of the reactor at different gas-mixture flow rates (the data are averaged over the reactor radius). It is seen that perfluoromethane is decomposed most effectively in the discharge zone of the reactor ($x < 4$ cm). In the afterdischarge zone, the rate of decomposition decreases and becomes zero at the end of the discharge tube. The calculations have shown that the CF_4 decomposition is terminated mainly due to the intense cooling of the flow by the discharge tube walls: 40–60% of the energy supplied to the flow in the discharge zone (this value is determined by the gas-flow rate) is lost to the end of the discharge tube. The gas is further cooled in the heat exchanger ($15 < x < 200$ cm).

It is seen that the degree of decomposition is a monotonically increasing function. This means that, in the afterbreakdown region, perfluoromethane is not even partially restored from the products of its decomposition. The last assumption is true only for initial mixtures in which $X_{O_2} > X_{CF_4}$. For mixtures in which oxygen is absent, the rate of CF_4 decomposition in the discharge region remains at the same level; however, the initial concentration of perfluoromethane reduces practically completely when it is cooled. Only a small part of perfluoromethane (~2–5%) can be transformed into such products as C_2F_6 .

Note that, even though the degree of decomposition of CF_4 in an oxygen-containing mixture in the heat exchanger does not change, in this region there occur intensive processes changing the chemical composition of the mixture (Fig. 6). However, the indicated change in the composition of the mixture is mainly due to the transformation of perfluoromethane decomposition products (CO , CO_2 , CF_3OF , CF_2O , and others) and the recombination of atomic components (O , N , and F).

Conclusions. A kinetic model of perfluoromethane decomposition including 172 elementary chemical reactions and taking into account the formation and decomposition of 51 chemical elements has been constructed. A stationary two-dimensional model of physicochemical processes occurring in a gas flow exposed to a microwave atmospheric-pressure discharge has been developed and realized in program codes. A series of numerical experiments have been conducted. The calculation data obtained are in good agreement with the corresponding experimental data.

NOTATION

A , preexponent, $cm^{3(q-1)}/sec$; b_C , amount of carbon in a component; c_p , specific heat capacity, $J/(kg \cdot K)$; E , energy, K ; G , gas-flow rate, liters/min; h , enthalpy, $J/mole$; k , rate constant, $cm^{3(q-1)}/sec$; N , number of chemical com-

ponents in the system; p , pressure, atm; q , order of reaction; R , universal gas constant, J/(mole·K); Re , Reynolds number; T , gas temperature, K; t , time, sec; u , gas velocity, m/sec; V , rate of diffusion of an element, m/sec; W , specific power of the discharge, W/m³; x, r , spatial coordinates, m; X , mole fraction of a component; Y , mass fraction of a component; α , degree of decomposition of perfluoromethane; β , exponent; γ , mole fraction of perfluoromethane; λ , gas-heat conductivity coefficient, W/(m·K); μ , molar mass, kg/mole; η , efficiency of purification; ρ , density, kg/m³; τ , characteristic time, sec; $\dot{\omega}$, rate of formation of a component, mole/(m³·sec). Subscripts: a, activation; i , index of the chemical element considered; min, minimum; max, maximum; 0, initial value.

REFERENCES

1. Y. Kabouzi, M. Moisan, J. C. Rostaing, et al., Abatement of perfluorinated compounds using microwave plasmas at atmospheric pressure, *J. Appl. Phys.*, **93**, 9483–9496 (2003).
2. M. N. Rolin, S. I. Shabunya, J. C. Rostaing, and J. Perrin, Simulation of microwave discharge in nitrogen at atmospheric pressure, in: *Proc. Int. Workshop "Nonequilibrium Processes in Combustion and Plasma Based Technologies,"* HMTI, Minsk (2004), pp. 59–63.
3. A. P. Chernukho, A. N. Migoun, S. A. Zhdanok, et al., Modeling of PFC destruction in atmospheric pressure microwave discharge, in: *Proc. Int. Workshop "Nonequilibrium Processes in Combustion and Plasma Based Technologies,"* HMTI, Minsk (2004), pp. 43–48.
4. A. Burcat, Third Millennium Ideal Gas and Condensed Phase Thermochemical Database for Combustion, Technion Aerospace Engineering (TAE), Report # 867, January 2001.
5. B. J. McBride, M. J. Zehe, and S. Gordon, NASA Glenn Coefficients for Calculating Thermodynamic Properties of Individual Species, NASA Report TP-2002-211556, September 2002.
6. P. J. Linstrom and W. G. Mallard, NIST Chemistry WebBook, NIST Standard Reference Database Number 69, March 2003, National Institute of Standards and Technology, Gaithersburg MD, 20899 (<http://webbook.nist.gov>).
7. A. A. Konnov, Development and validation of a detailed reaction mechanism for the combustion of small hydrocarbons, in: *Proc. 28th Int. Symp. on Combustion*, Edinburgh (2000), p. 317.
8. G. P. Smith, D. M. Golden, M. Frenklach, N. W. Moriarty, B. Eiteneer, M. Goldenberg, C. T. Bowman, R. K. Hanson, S. Song, W. C. Gardiner Jr., V. V. Lissianski, and Q. Zhiwei, http://www.me.berkeley.edu/gri_mech/.
9. J. A. Miller and C. T. Bowman, Mechanism and modeling of nitrogen chemistry in combustion, *Prog. Energy Combust. Sci.*, **15**, 287–338 (1989).
10. H. Wang and M. Frenklach, A detailed kinetic modeling study of aromatics formation in laminar premixed acetylene and ethylene flames, *Combust. Flame*, **110**, 173–221 (1997).
11. K. J. Hughes, T. Turányi, A. Clague, and M. J. Pilling, Development and testing of a comprehensive chemical mechanism for the oxidation of methane, *Int. J. Chem. Kinet.*, **33**, 513–538 (2001).
12. J. C. Leylegian, D. L. Zhu, C. K. Law, and H. Wang, Experiments and numerical simulation on the laminar flame speeds of dichloromethane and trichloromethane, *Combust. Flame*, **114**, 285–293 (1998).
13. A. A. Turnipseed, S. B. Barone, N. R. Jensen, D. R. Hanson, C. J. Howard, and A. R. Ravishankara, Kinetics of the reactions of CF₃O radicals with CO and H₂O, *J. Phys. Chem.*, **99**, 6000 (1995).
14. Y. Kabouzi, M. D. Calzada, M. Moisan, et al., Radial contraction of microwave-sustained plasma columns at atmospheric pressure, *J. Appl. Phys.*, **91**, 1008–1019 (2002).